Robust Video-oculography for Non-invasive Autonomic Nerve Quantification

Masaru Kiyama, *Student Member, IEEE*, Hitoshi Iyatomi, *Member, IEEE*, and Koichi Ogawa, *Member, IEEE*

***Abstract*— A relationship between autonomic nerves activity and depression or Alzheimer's disease has been reported. The quantification of autonomic nerves is expected to serve as a tool for quantifying the of severity of the disease or for early detection. Video-oculography is known as a non-invasive and reliable procedure of measurement of pupil response and is used in clinical practice. However, measuring the transition of pupil areas accurately is often difficult due to eyelid overlap, effects of blinking, eyelashes etc. Current video-oculography only performs thresholding to split pupil area and backgrounds and therefore sometimes has difficult in measuring accurate transitions of pupil reflex. In this study, we developed a robust and accurate method to measure the transition of pupil size. The proposed method introduces an interpolation process using an active contour model and ellipse estimation with selection of reliable contour points and attains robust measurement of pupil area against the abovementioned difficulties. We confirmed our method achieved an extraction accuracy of 98.3 % in precision and 98.9% in recall in average on the tested a total of 8,518 image frames from 30 movies.**

***Index Terms*— autonomic nerves, oculography, pupil reflex**

I. Introduction

Autonomic nerves controls human organs. Evaluation of activity of autonomic nerves is expected to serve for the quantification and/or early detection of depression or Alzheimer's disease [1][2]. Evaluation of autonomic nerves are roughly categorized into two types. The first are methods using micro-neurography, which measures the activity of autonomic nerves directly [3] and the others are indirect methods that evaluate organs controlled by them [4]. The former requires invasive examination being borne by the patient while the others are capable of non-invasive examinations. Since those methods are relatively easy in clinical practice and inflict much less stress for the patients, they have been investigated widely and the methods monitoring and analyzing cardiac beats are commonly used.

Oculography or video-oculography [5] evaluates two types of smooth muscles innervated by autonomic nerves. A patient is given an impulse light stimulation on his/her pupil and an oculography monitors a transition of his/her pupil reflex.
A pupil is controlled by two types of smooth muscles: dilator pupillae muscles and sphincter pupillae muscles. The former are innervated by a sympathetic nerve and cause dilation a pupil and the latter are innervated by a parasympathetic nerve and cause pupil constriction. So, the oculography evaluates the activity of these two opposite rolled nerves by monitoring a transition of pupil reflex.

Faculty of Engineering, Hosei University, 3-7-2 Kajino-cho Koganei, 184-8522, Tokyo, Japan (phone: 81-42-387-6217; fax: 81-42-387-6381; e-mail:iyatomi@hosei.ac.jp).

Oculography has an advantage in inspection time compared with methods utilizing cardiac monitoring. However, currently used video-oculography only performs thresholding to split pupil area and backgrounds from a movie and therefore, it cannot track accurate transition of pupil size where pupil area in an image frame is absent due to being covered by an eyelid (commonly seen) and especially affected by blinking, and has an over-estimation by eyelashes, etc.

Much research on measuring pupil reflex have been proposed [6]-[8]. Sakashita et al. [6] estimate pupil area by approximating an ellipse based on an inscribed parallelogram from tentatively extracted pupil area. This method is fast and interpolates abovementioned deficits or over-extraction, however it has a difficulty when the defect of the contour of the pupil exceeds around 30%. Moriyama et al. [7] prepared pupil models and estimated a pupil using a pattern matching strategy. This method is robust against noise and attains accurate estimation but requires the construction of a patient-specific pattern and initial alignment.

The proposed method introduces an interpolation process which includes an active contour model and ellipse estimation with selection of reliable contour points corresponding to the effect by eyelids, eyelashes, spot-light noise, etc. and a comparison process which considers the past frames addresses large deficits of pupil area occurring from blinking.

II. Measurement device and movies

A. Development of measurement device

We built a video-oculography scope in accordance with the Pharmaceutical Affairs Act (Fig.1). The key components of our scope are the infrared camera, infrared diode for illumination, white LED for light stimulation on pupil, polarization filter in order to reduce spot noise of the video image, and USB interface to computer. The scope records a movie for a set amount of time including pupil reflex caused by light stimulation. Our pupil area estimation algorithm on a USB connected computer determines pupil area with interpolation processes in each image frame.

B. Movies

In this study, we used a total of 30 movies from 6 volunteer normal men captured by our scope. The property of each movie has 640x480 pixels in resolution, 8-bit gray scale and the frame rate of 30. The duration of light stimulation for pupil is 0.5 second (the same length used in video-oculography in clinical practice) in each movie. Each movie includes at least one blink (1.33 ± 0.55 times). The total number of calculated image frame was 8,518 and the distribution of the video length was 9.46 ± 1.23 seconds (means $\pm$ SD).

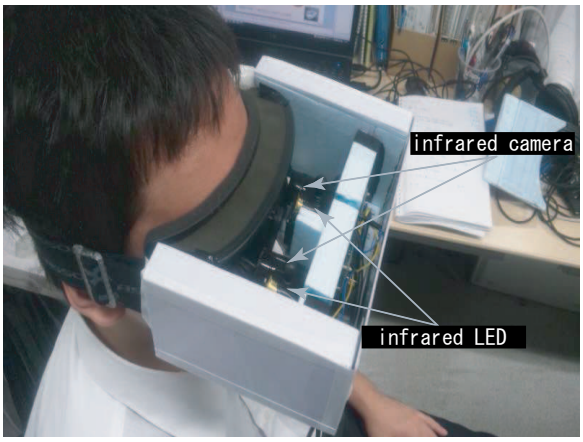

Fig. 1. Developed oculography scope

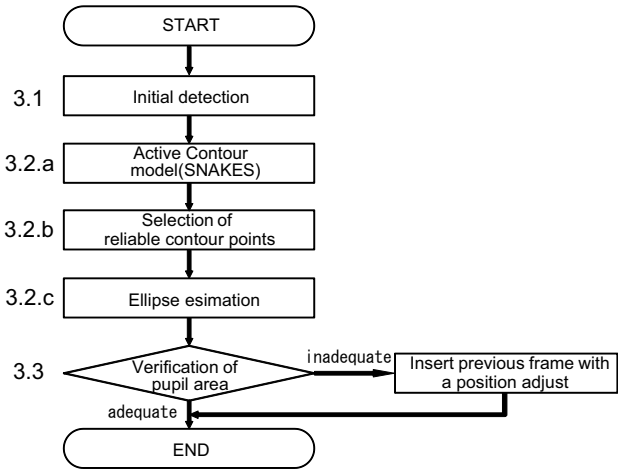

Fig. 2. Overview of the proposed pupil area measurement algorithm

III. Measurement of pupil area

The overview of the proposed pupil area measurement algorithm for each captured image is shown in Fig.2. Firstly, we determined an initial pupil area by thresholding. Then, we used (1) an active contour model (snakes) [9] to reduce the false extraction mainly caused by eyelashes and (2) an ellipse estimation with selection of reliable contour points to handle issues caused by eyelids and blinking. In addition, (3) substitution process was applied as necessary based on a comparison with several former frames for cases where most of the pupil area is absent due to blinking, etc. The following sections describe them in detail.

A. Pre-processing and initial extraction

An infrared illumination introduces undesirable bright spots on a captured image and they sometimes cause serious effects on measuring a pupil. We introduced a polarization filter at the end of our infrared camera to reduce the abovementioned effect and performed gamma correlation ($\gamma = 1.7$) to address darkened image by the filter. As an initial extraction of pupil area, we performed a thresholding with the value θ to split a pupil area from the background. In this study, we determined $\theta = 30$ based on preliminary experiments. Then, we set an ROI in the middle of an image and the largest region inside the ROI was regarded as the initial pupil area.

B. Determination of pupil area by interpolation

An initially determined pupil area is often affected by the above-mentioned noises such as remaining bright spot, deficit by eyelid, blink, and effects by eyelashes or eyelash linear. In this phase, we determined the pupil area with the following three steps.

1) Estimation of the pupil contour: Eyelashes and especially eyelash liner absorb infrared as well as pupil. Hence, only performing a simple thresholding causes a false extraction of those areas. In addition, pupil area is overlapped by eyelid during a blinking. In this step, we estimate the candidates of the pupil contour based on the initially determined pupil area using the active contour model [9] (Fig.3(a)).

The active contour model is one of the contour detection methods. The algorithm firstly spaces out a closed curve being composed of several contour points s near the target object (i.e. initial extraction of the pupil) on the image. Then it transforms the curve (i.e. set of contour points) iteratively with reference to the edge characteristics, smoothness, intensity of the target and so on. Finally the algorithm determines the shape of the target object. In this study, we determined the energy function of the active contour model as equation (1) and transformed contour points s iteratively to minimize the function.

$$E_{snakes} = \int_0^1 E_{int}(v(s)) + E_{image}(v(s))ds \qquad (1)$$

where,

$$E_{int}(v(s)) = \frac{1}{2}\alpha(s)|v_s(s)|^2 + \beta(s)|v_{ss}(s)|^2 \quad (2)$$

$$E_{image}(v(s)) = -\omega(s)|\nabla(v(s))|. \quad (3)$$

$E_{int}(v(s))$ is the internal energy determined by the length $v_s(s)$ and the smoothness $v_{ss}(s)$ of the contour. $E_{image}(v(s))$ is the image energy calculated from the edge intensity. In this study, the number of the contour points s constituting a closed curve was 40, weighting factors of each energy was determined as $\alpha(s) = 1.0, \beta(s) = 1.25, \omega(s) = 1.0$ based on the results of preliminary experiments.

2) Selection of reliable contour points: The estimated contour candidates by the active contour model sometimes include inadequate points. In order to eliminate those points and estimate correct contour candidates, we developed candidate selection algorithm as follows:

- Connect all contour points determined in the former step with a straight line.
- Assume an arbitrary contour point in the left hemicycle p_i, find the vertically same position of p_i on the connected line or contour points in the right hemicycle q_i, and calculate their centroid $c_i : (x_i, y_i)$. Calculate all centroid points $c_i (1 \leq i \leq n)$ from all p_i (Fig.3(b)). We treat all p_i and q_i as candidates of pupil contour (i.e. total $2n$) at this time.

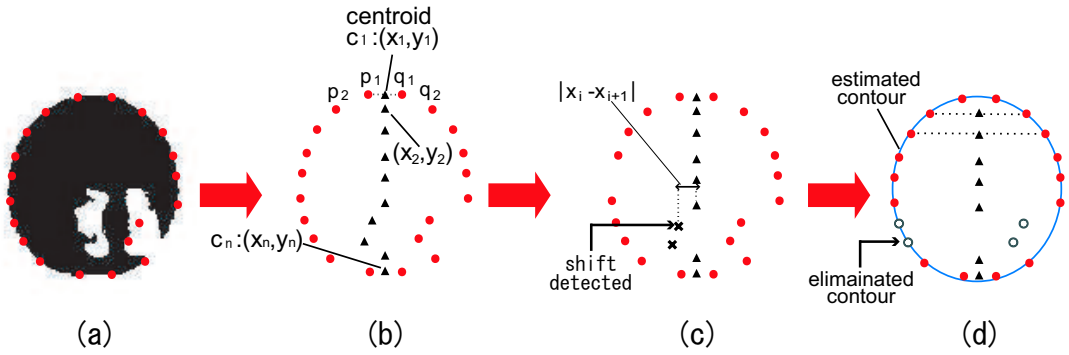

Fig. 3. Selection of reliable contour points

- Investigate the shift amount in horizontal direction: $\mid x_i - x_{i+1} \mid$ $(\forall i)$. If not negligible shift is detected, $\mid x_i - x_{i+1} \mid > \xi_x$ (Fig.3(c)), we assume the current pupil area(s) have deficits and accordingly eliminate contour points p_i and q_i from the candidates (Fig.3(d)). In this study, we determined ξ_x was 2% of the pupil size. All remaining contour points are treated as "reliable".

3) Ellipse estimation using reliable contour points: Finally, the pupil area is determined in this phase by means of an ellipse estimation using a least squares method with the reliable contour points (Fig.3(d)). Ellipse parameters determined here are the position, major and minor axes of the pupil and its rotation.

C. Verification of extraction with former frames

We examine the validity of the determined pupil area by the comparison with the results of five former frames. Let the major length of the ellipse l, ratio of the major and minor axes r, and the corresponding five formers as l_i and r_i (i=1,2,$\cdots$ 5), respectively. If the target image frame meets both of the following conditions, $\mid r - r_i \mid \geq r_{diff}$ and $\mid l - l_i \mid \geq l_{diff}$ at least three times in the last five frames, the extraction of the pupil in the target frame is considered as inadequate. In this case, the extraction result (i.e. pupil size and shape) of the adjacent frame is used and the center position of the pupil (g_x, g_y) is determined, referred to method proposed by Kim et al. [8]. The position is determines as: (i) find the bottom position of the pupil (b_x, b_y) where b_x is the x (horizontal) coordinate of the gravity point and b_y is the y (vertical) coordinate of the bottom pixel of the tentative extraction of the pupil in the current frame, respectively. (ii) investigate the radius of the pupil size in vertical direction l_y in the adjacent frame. (iii) determine the center of the pupil location $(g_x, g_y) = (b_x, b_y + l_y)$. (positive in y direction indicates upper direction)

In this experiment, we used $r_{diff} = 0.05, l_{diff} = L/120$ based on preliminary experiments, where L is the width of image frame.

IV. Experiment

We evaluate the performance of our method with captured movies as described in section II. In order to perform a quantitative evaluation, we manually specified pupil area for all image frames and used them as gold standard. As

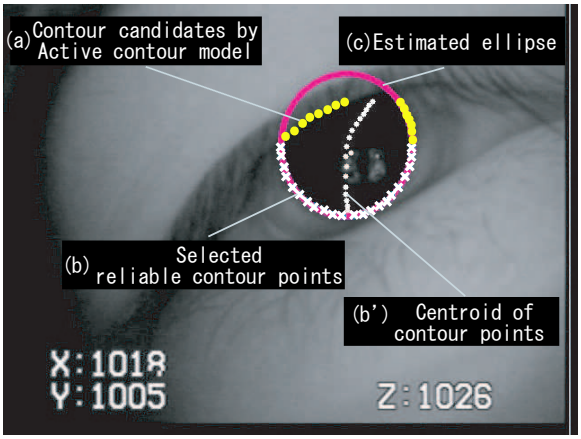

Fig. 4. Explanatory diagram of the interpolation phase

the evaluation criteria, we use precision and recall in our studies. In general terms, precision is a measure of the accuracy of the extraction (estimation, determination), or whether a chosen pixel is actually part of the pupil. Recall is a measure of how much of the pupil is covered by the extraction, or how many actual pupil pixels were chosen by the extraction. Since precision and recall are trade-off criteria, we also use F-measure criterion as follow to evaluate general extraction performance. We compared the performance with Sakashita's method [6] and the method with just a thresholding as a reference.

V. Result

Fig.4 shows an example how our method estimates the pupil area. In this example, pupil area is affected by eyelashes and eyelid and therefore conventional video-oculography performing simple thresholding cannot estimate adequate pupil size. The active contour model successfully reduced the infection of eyelashes, however it extracted not the appropriate pupil area but the contour of the pupil partially hidden by eyelid (Fig.4(a)). In the selection of reliable contour points step, we selected 24 reliable contour points (Fig.4(b)) by considering the centroid of the contour points (Fig.4(b')). Then pupil area was reasonably determined by ellipse estimation using reliable pupil contour (Fig.4(c)).

Fig.5 shows typical examples that pupil areas are affected by some issues, (a) and (b): eyelashes, (c) and (d): eyelid and

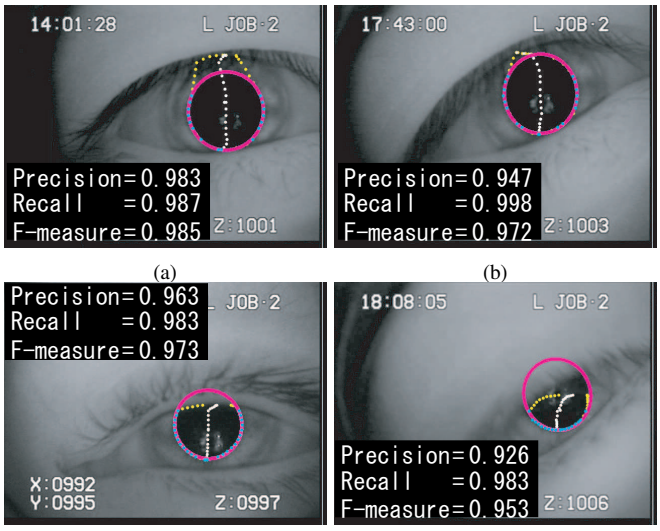

Fig. 5. Examples of pupil area estimation

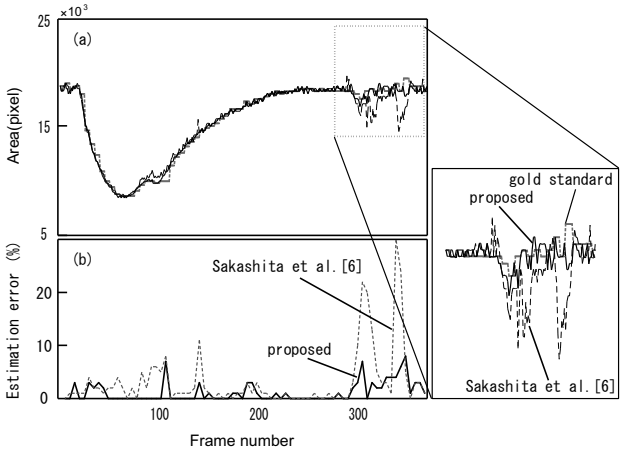

Fig. 6. Traced pupil reflex

blink. Fig.6 illustrates an example of a transition of detected pupil area (upper) and its estimation error (lower). As we can see our method successfully determined pupil area and track a transition of pupil size appropriately.

The estimation performance was summarized in Tables 1 and 2. The proposed method achieved a precision of 98.31%, recall of 98.86%, and F-measure of 0.9886 in average. Also from the distribution of F-measure, 99% of the image frames exceed the F-measure of 90. Our results showed superior results compared to method [6] or thresholding. The average processing time was 0.09 sec/frame using Panasonic Let's Note S9 notebook PC (Intel Core i5-520M processor).

VI. Discussion and Conclusion

In video-oculography, physicians diagnose the severity of disease using a transition of pupil size as shown in Fig.6. From this point of a view, we think an acceptable error in estimating pupil size is around 5% (is equivalent to 2.4% error in a diameter) in average and around 10% (also 4.9% in a diameter) at maximum. Our method successfully estimated pupil area in most cases (average F-measure is 0.9886) and only 1.0% of the image frame showed F-measure score lower than 90 (conventional method [6] and thresholding missed 6.8% and 12.8%, respectively). As from Fig.6(d), estimation error of 5% (i.e. F-measure is around 0.95) is not discernible in visual.

We can see that our method successfully estimated accurate pupil area for almost all cases and it is fast enough for use in clinical practice. We consider our automatic algorithm finding related diseases in early stage or quantify it in near future.

TABLE I

Comparison of pupil area estimation performance

Method / Criteria	precision (%)	recall (%)	F-measure
Proposed	98.31	98.86	0.9886
Sakashita et al.[6]	94.74	94.29	0.9484
thresholding	96.53	87.21	0.9139

TABLE II

Statistics of pupil detection accuracy

Method / F-measure†	95+ (%)	90+ (%)	85+ (%)	80+ (%)
Proposed	95.74	99.03	99.47	99.68
Sakashita et al.[6]	84.16	93.28	95.19	96.53
thresholding	56.67	87.17	93.69	96.18

†: Cumulative percentages of the number of image frames exceed the F-measure.

References

[1] S.Elmstahl, M.Petersson, B.Lija, S-M.Samuelssob, I.Rosen, and L.Bjuno, "Autonomic Cardiovascular Responsesto Tilting in Patients with Alzheimer's Disease and in Healthy Elderly Women", Age Ageing Vol.21, No.4, pp301-307, 1992.

[2] M.E.Jarrett, R.L.Burr, K.C.Cain, V. Hertig, P.Weisman and M.M.Heitkemper,"Anxiety and Depression Are Related to Autonomic Nervous System Function in Women with Irritable Bowel Syndrome," Digestive Diseases and Sciences, Vol.48, No.2, pp.386-394, 2003.

[3] B.A.Kingwell, J.M.Thompson, D.M.Kaye, G.A.McPherson, G.L.Jennings and M.D.Esler, "Heart Rate Spectral Analysis, CardiacNorepinephrine Spillover, and MuscleSympathetic Nerve Activity During HumanSympathetic Nervous Activation and Failure," Circulation, Vol.90, 234-240, 1994.

[4] J.Sztajzel, "Heart rate variability: a noninvasive electrocardiographic method to measure the autonomic nervous system," Swiss Medical Weekly, Vol.134, pp.514-522, 2004.

[5] D.Pittasch, R.Lobmann, W. Behrens-Baumann, and H. Lehnert,"Pupil Signs of Sympathetic Autonomic Neuropathy in Patients With Type 1 Diabetes," Diabetes Care September, Vol.25, No. 9, pp.1545-1550, 2002.

[6] Y.Sakashita, H.Fujiyoshi, Y.Hirata, H. Takamaru, and N.Fukaya, "Real-Time Measurement of Cycloduction Movement Based on Fast Ellipse Detection," Electronics and Communications in Japan, Vol.92, No.11, pp.9-18, 2009.

[7] T.Moriyama, T.Kanade, T.J.Xiao, and J.F.Cohn, "Meticulously Detailed Eye Region Model and Its Application to Analysis of Facial Images," IEEE Trans. on Pattern Analysis and Machine Intelligence ,Vol.28, No.5, pp.738-752, 2006.

[8] S.C.Kim, K.C.Nam, W.S.Lee, and D.W.Kim, "A new method for accurate and fast measurement of 3D eye movements, " Medical Engineering & Physics Vol.28, pp.82-89, 2006.

[9] M. Kass, A.Witkin, and D.Terzopoulos,"Snakes Active contour models," International Journal of Computer Vision, Vol.1, No.4, pp.321-331, 1988.